

MLP-SLAM: Multilayer Perceptron-Based Simultaneous Localization and Mapping With a Dynamic and Static Object Discriminator

Taozhe Li¹ and Wei Sun²

Abstract—The Visual Simultaneous Localization and Mapping (V-SLAM) system has seen significant development in recent years, demonstrating high precision in environments with limited dynamic objects. However, their performance significantly deteriorates when deployed in settings with a higher presence of movable objects, such as environments with pedestrians, cars, and buses, which are common in outdoor scenes. To address this issue, we propose a Multilayer Perceptron (MLP)-based real-time stereo SLAM system that leverages complete geometry information to avoid information loss. Moreover, there is currently no publicly available dataset for directly evaluating the effectiveness of dynamic and static feature classification methods, and to bridge this gap, we have created a publicly available dataset containing over 50,000 feature points. Experimental results demonstrate that our MLP-based dynamic and static feature point discriminator has achieved superior performance compared to other methods on this dataset. Furthermore, the MLP-based real-time stereo SLAM system has shown the highest average precision and fastest speed on the outdoor KITTI tracking datasets compared to other dynamic SLAM systems. The open-source code and datasets are available at <https://github.com/TaozheLi/MLP-SLAM>.

Index Terms—Multilayer Perceptron, Dynamic SLAM, Machine Learning

I. INTRODUCTION

Visual Simultaneous Localization and Mapping (V-SLAM) is designed to achieve precise ego-localization and construct an accurate map of the surroundings using only the camera sensor. The camera sensor is light-weight and cost-effective, while capable of capturing high resolution images. V-SLAM has played a crucial role in various fields, including robotics, space exploration, and autonomous driving. For example, accurate mapping and precise ego-localization significantly impact the navigation and decision-making processes of autonomous driving systems. However, most existing SLAM systems are heavily reliant on the assumption of a static world, including state-of-the-art (SOTA) systems such as ORB-SLAM2 [1], ORB-SLAM3 [2], LSD-SLAM [3] and Direct Sparse Odometry [4]. These systems typically perform with high precision in environments with predominantly static objects. Nevertheless, their precision deteriorates when deployed in dynamic environments, which are common in real world scenarios. Research efforts aimed at addressing the degradation of SLAM systems in dynamic environments can

be categorized into three parts. Part I focuses only on geometry methods, which involve classifying feature points based solely on geometric information. This information includes epipolar error, reprojection error, image intensity, depth, and optical flow, as demonstrated in works such as [5]. Part II, exemplified by works like DynaSLAM [6], leverages prior class information obtained from object detection models or semantic segmentation models to identify features within bounding boxes or masks of objects belonging to dynamic classes as outliers, which are then discarded during camera pose estimation. While these approaches partially mitigate the degradation of SLAM systems in dynamic environments, their effectiveness is limited. For instance, features extracted from stationary parked cars on the roadside may be erroneously removed, despite their static nature and potential value in estimating camera pose, leading to information loss. In Figure 1, a qualitative comparison is presented between our Multilayer Perceptron (MLP)-based discriminator for dynamic and static feature points and the method proposed in DynaSLAM, using a snapshot from the Kitti tracking dataset [7]. The top image displays the results of our method, while the bottom image shows the results of the method in DynaSLAM. In the left image, the method in DynaSLAM categorizes feature points on the highway guardrail as dynamic, whereas our method correctly predicts them as static. In the right image, numerous static feature points associated with parked cars on the roadside are misclassified as dynamic by the method in DynaSLAM, whereas our method correctly identifies them as static. This evidence supports the effectiveness and reliability of our method. Part III represents the current mainstream approach, which combines methods from Part I and Part II, as demonstrated in works such as DynaSLAM, CFP-SLAM [8], PointSLOT [9], VDO-SLAM [10], and D-SLAM [11], by initially acquiring prior class information through deep learning models such as object detection models or semantic segmentation models. The most prevalent deep learning models utilized in the Simultaneous Localization and Mapping (SLAM) domain are from the YOLO series, known for their high precision and rapid processing speed, such as YOLOv5 [12] and YOLOACT [13]. Subsequently, leveraging the prior class information obtained from these models, geometric methods are employed to eliminate dynamic feature points. These geometric aspects encompass various factors, including epipolar error, re-projection error, image intensity, depth, and velocity (if tracking dynamic object pose). However, a significant portion of the existing methodologies in Part III only utilize partial geometric information. For instance, some methods solely

¹Taozhe Li is a graduate student at the School of Aerospace and Mechanical Engineering, University of Oklahoma, Norman, OK, US. Taozhe.Li-1@ou.edu

²Wei Sun is an Assistant Professor at the School of Aerospace and Mechanical Engineering, University of Oklahoma, Norman, OK, US. wsun@ou.edu

focus on epipolar error [14], re-projection error [9], or a combination thereof [8]. These approaches are commonly employed in the dynamic SLAM field. Nevertheless, these methods often require manual parameter tuning, lack generality, and are excessively laborious to fine-tune. Furthermore, the evaluation of methods distinguishing between dynamic and static feature points is typically conducted indirectly through SLAM field metrics, as there is a lack of publicly available datasets specifically designed for this classification task. This indirect evaluation method tends to be inaccurate and unreliable due to the randomness in the Random Sample Consensus (RANSAC) process in camera pose estimation within the SLAM system.

To address the aforementioned gaps, this letter introduces a MLP-based real-time stereo SLAM system and establishes publicly available datasets to classify dynamic and static feature points. The contributions outlined in this work are as follows:

- We introduce an open-source MLP-based real-time stereo system designed to enhance performance in dynamic environments. This system leverages comprehensive geometry information and eliminates the need for manual parameter configuration. To the best of our knowledge, it is the first time that a MLP machine learning method is applied to SLAM system as a dynamic and static feature points discriminator.
- We have constructed publicly available datasets comprising more than 50,000 feature points sourced from the KITTI tracking datasets [7] for the purpose of training and testing dynamic and static feature points discriminators. The efficacy of it can be evaluated directly with this dataset.

II. RELATED WORK

A. Dynamic SLAM

The emergence of DynaSLAM has garnered significant attention in the Visual Simultaneous Localization and Mapping field since its release. This approach identifies feature points located within the semantic mask of potential moving objects as outliers and subsequently discards them. While it has shown improvements in the KITTI tracking sequences 01, 08, and 09 compared to ORB-SLAM2, this method may misrepresent dynamic and static objects, as shown in Figure 1. Moreover, DynaSLAM is plagued by high latency issues attributed to its reliance on the computationally intensive deep learning model MaskRCNN [15] for generating semantic segmentation masks. Subsequent research endeavors have aimed to address the degradation of SLAM systems in dynamic environments. For instance, work CFP-SLAM[9] introduced a Moving Objects Recognition (MOR) approach to differentiate between dynamic and static feature points by utilizing the re-projection error. In comparison, work [8] employs a DBSCAN[16] clustering machine learning technique to filter out features within bounding boxes that belong to the background and then employ a geometric method that incorporates geometric information such as re-projection error and epipolar error to distinguish dynamic

and static feature points. An inherent limitation in [9] and [8] is the requirement of the establishment and tuning of manual parameters, which restricts the application scenarios and diminishes the generality of the SLAM system. Furthermore, these approaches do not fully leverage geometric information. The VDO-SLAM[10] and DynaSLAM II[17] are extensions of DynaSLAM, with DynaSLAM II representing the current state-of-the-art (SOTA) in camera motion estimation. Both works initially estimate the camera pose using feature points outside the potential dynamic class semantic mask, akin to the approach in DynaSLAM. Subsequently, they estimate the object pose for each frame and optimize the camera and object poses simultaneously through Bundle Adjustment (BA) factor graph. However, these methodologies encounter high latency issues due to data association challenges between dynamic objects and object pose estimation. Additionally, the precision of object pose estimation is compromised by the limited number of matched feature points and the quality of feature matching for each object.

B. Multilayer Perceptron

Multilayer Perceptron (MLP) [18] is commonly utilized as a tool for classification tasks, and it has been effectively employed in artificial intelligence, particularly in the field of computer vision. One of the most renowned applications is the utilization of MLP to address the problem of recognizing handwritten digits [19]. Another application is the diagnosis systems in the medical field [20]. The MLP primarily comprises three components. The first component is the input layer, which is responsible for receiving the features of each data point. The second component is the hidden layer, where the number of nodes in each layer and the depth of the hidden layer significantly influence its performance. Specifically, the model can handle more complex tasks with a greater depth in the hidden layer and more nodes in each hidden layer. The third component is the output layer, which can be viewed as the post-processing of results from the hidden layers to fulfill various tasks. In the field of Simultaneous Localization and Mapping (SLAM), studies [21], [5], [22] applied the MLP to decode grid features into occupancy values in the mapping part. To the best of our knowledge, the method introduced in our letter is the first instance of applying the MLP as a discriminator for dynamic and static feature points in the SLAM domain.

III. OVERVIEW

A. Notations in SLAM

World and camera coordinates are denoted by $\{W\}$ and $\{C\}$ respectively. ${}^tX_i^B$ describes the i_{th} 3D cloud point at time t and located in the coordinate of $\{B\}$, $B \in \{W, C\}$. Moreover, tP_i marks the i_{th} point in the image plane, and the operation $\pi(\cdot)$ represents projecting an 3D point cloud from camera coordinates into the image plane. i.e. ${}^tP_i = \pi({}^tX_i^C)$. Besides, the translation matrix ${}^tT_{CW} = \begin{bmatrix} {}^tR_{CW} & \mathbf{t}_{CW} \\ 0 & 1 \end{bmatrix} \in SE(3)$ is used to describe a transformation from the world

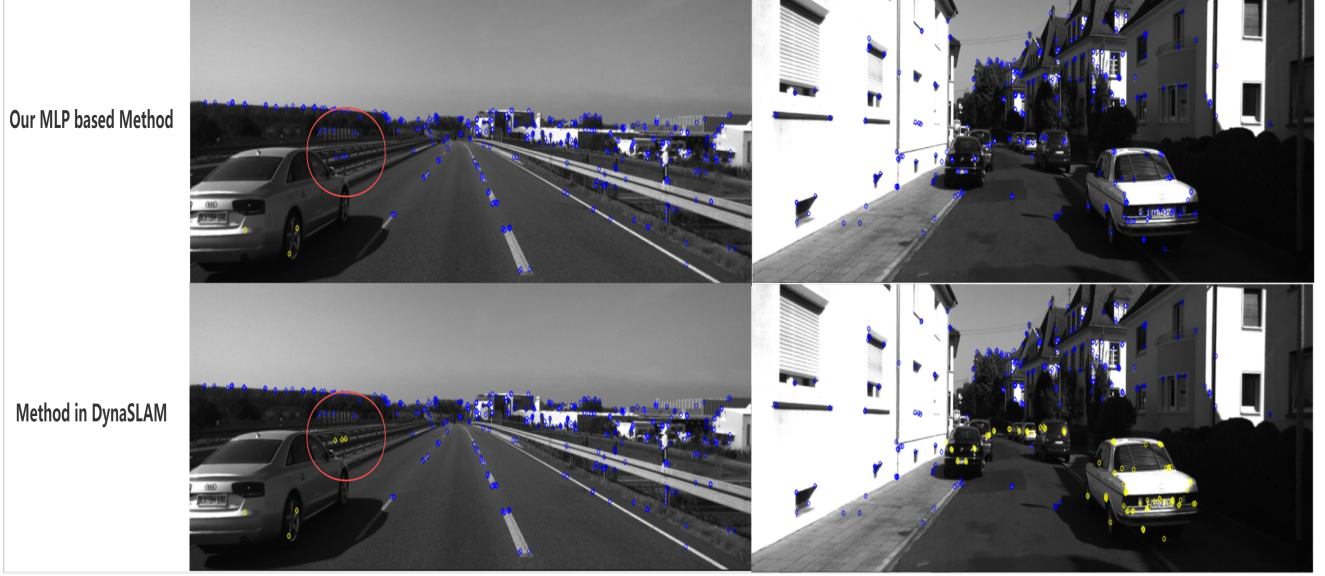


Fig. 1. Qualitative comparison between our method and method in DynaSLAM. The static feature point is represented by a blue circle, while the dynamic feature point is represented by a yellow circle. The top image displays the results of our method, while the bottom image shows the results of the method in DynaSLAM. In the left image, the method in DynaSLAM categorizes feature points on the highway guardrail as dynamic, whereas our method correctly predicts them as static. In the right image, numerous static feature points associated with parked cars on the roadside are misclassified as dynamic by the method in DynaSLAM, whereas our method correctly identifies them as static.

coordinate $\{W\}$ to the camera coordinate $\{C\}$. The matrix ${}^tR_{CW} \in SO(3)$ denotes the rotation part and the \mathbf{t}_{CW} denotes the translation part of ${}^tT_{CW}$. The essential matrix between two consecutive frames is denoted by E . The i_{th} feature point is denoted by x_i , and its depth is represented by d_i .

B. Camera Pose Estimation

In the camera pose estimation process, we search the static feature point correspondences among consecutive frames to avoid the impact of dynamic objects. More specifically, we first do a coarse estimation with feature points that are outside of the bounding box which belongs to potential dynamic objects, as well as the static feature points inside the bounding box that are identified by the Depth Filter Module. And then we do a fine estimation where static feature points on potential dynamic objects are filtered by the MLP model and they will also be used for camera pose estimation. The camera pose is acquired through minimizing the re-projection error of static feature point correspondences, which is described by:

$${}^tT_{CW} = \arg \min_{{}^tT_{CW}^*} \sum_i^N \rho(\|{}^t e_i\|_2^2), \quad (1)$$

where

$${}^t e_i = {}^t P_i - \pi({}^t T_{CW} {}^{t-1} X_i^W), \quad (2)$$

and the operation $\rho(\cdot)$ is a robust kernel function for reducing impact of feature points with big error, and N denotes the number of static feature correspondences.

C. Notations in MLP

The generated input feature for each feature point x_i is represented by $v_i \in R^3$. Each generated feature v_i consists of three parts, which are e_I , e_D and e_{Re} . i.e. $v_i = \begin{Bmatrix} e_I \\ e_D \\ e_{Re} \end{Bmatrix}$. The e_I , e_D and e_{Re} represent the image intensity error, epipolar error and re-projection error respectively. They are computed as follows

$$e_I(x_1, x_2) = \|I(P_1) - I(P_2)\|_2^2, \quad (3)$$

$$e_D(E, x_1, x_2) = \frac{P_2^T E}{\|P_2^T E\|} \cdot P_1, \quad (4)$$

$$e_{Re}(R_{12}, t_{12}, x_1, x_2) = \|\pi(R_{12}\pi(P_2, d_2)^{-1} + t_{12}) - P_1\|_2^2. \quad (5)$$

We use operation $M(\cdot)$ to denote applying MLP model for classifying dynamic and static feature points. The prediction result and the label are denoted by $y^p \in R^2$ and $y^t \in R^2$. And the label of each feature point is denoted by c_i . For our problem, the label c_i equals 0 or 1. We used 0 to indicate static class and 1 for dynamic class. Thus, the MLP model predicted process can be described by

$$c_i = \operatorname{argmax}(y_i^p), \quad (6)$$

where

$$y_i^p = M(v_i). \quad (7)$$

D. Loss function

There are lots of different types of loss function. They all operate by quantifying the difference between a model's pre-

dictions and actual target. With the loss function, the gradient can be calculated to update model parameters through back propagation. In this letter, *Binary Cross-Entropy (BCE) Loss* is chosen as loss function for MLP to classify dynamic and static feature points. The entropy indicates a calculation of the degree of randomness or disorder within a system. The cross-entropy measures the differences between two probability distributions that can be used to identify an observation. The BCE Loss is used for measuring the difference between the prediction of machine learning algorithm and the actual target prediction that is calculated from the negative value of the summation of the logarithm value of the probabilities of the predictions made by the machine learning algorithm against the total number of data samples. We use y_t and y_p to present true target and prediction of Multilayer perceptron model respectively. The mathematical equation for *Binary Cross-Entropy (BCE) Loss* is presented as following:

$$BCE(y_i^t, y_i^p) = -y_i^t * \log(y_i^p) - (1 - y_i^t) * \log(1 - y_i^p) \quad (8)$$

IV. PROPOSED METHOD

The diagram of our MLP-based stereo real-time SLAM system is shown in Figure 2. Initially, the input stereo images undergo feature extraction. Subsequently, object detection and tracking are performed on the left image. The process then moves to a coarse estimation stage where features outside the bounding box of potential dynamic objects, and the background static features within the bounding box that are filtered by the Depth Filter Module, are used for coarse camera pose estimation. Then each feature point x_i that is inside the bounding box and not filtered by the Depth Filter Module generates an input feature v_i using formulas (3), (4), and (5). The MLP model assigns a label c_i to each feature point to distinguish static and dynamic feature points. Finally, all static feature points are used for fine camera pose estimation. In this section, details of each module and our collected dynamic and static feature points classification dataset will be elaborated.

A. Depth Filter Module

We opt for object detection and tracking models over semantic segmentation models in our SLAM system to reduce latency, as the latter typically requires more computational resources. However, object detection models produce less accurate bounding boxes compared to mask from semantic segmentation models. To address this issue, we introduce the *Depth Filter Module* to remove background features within the bounding box, classifying them as static. The process of the Depth Filter Module is as follows: Initially, we calculate the average depth μ_d of all feature points within the bounding box, provided there are a sufficient number of feature points. Subsequently, we calculate the standard deviation δ_d of these points. Any feature points falling outside the range $[\mu_d - \eta\delta_d, \mu_d + \eta\delta_d]$ are eliminated from the potential dynamic feature point set and treated as static in coarse estimation stage. Here, η represents a constant value that describes the degree of deviation from the average depth value.

B. Coarse Estimation Module

Stereo images are used for ORB feature extraction initially. The left image is utilized for object detection and tracking using YOLOv7 [23] and Deep Sort [24]. In comparison to CFP-SLAM, which uses an extended Kalman filter (EKF) and Hungarian algorithm to compensate for missed object detection, we employ Deep Sort for a more effective implementation of the same function. Leveraging class information from the object detection model, we utilize the *Depth Filter Module* to treat background features as static points and combine them with all static feature points outside of the bounding boxes to estimate the camera pose by minimizing the re-projection error as in equation (1).

C. Multilayer Perceptron Module

This section details the construction and deployment of a MLP model to effectively differentiate between dynamic and static feature points.

Before deploying the MLP model to classify dynamic and static feature points, a sufficient dataset is needed for training. Therefore, a dataset containing dynamic and static feature points is created. Details of the dataset collection process are provided in Section IV-E. Once an adequate dataset is available, the structure of the MLP model needs to be designed. The MLP model consists of three parts: the input layer, the hidden layer, and the output layer. The input layer's number of nodes corresponds to the dimension of the input feature, which is three in this case: the image intensity error e_I , the epipolar error e_D , and the re-projection error e_{Re} . Previous work has often overlooked some of these features, leading to incomplete information. After setting up the input layer, our attention shifts to the hidden layer, which is crucial for the MLP model's classification performance. In this study, a two-layer hidden layer with ten nodes each is constructed. The final step is to create the output layer. In our case, an output layer with two nodes that denotes the dynamic and static classes is utilized.

With a constructed MLP model and sufficient data, training is essential for successful classification of dynamic and static feature points. The first step involves applying zero mean normalization to the datasets. Although min-max normalization is attempted to scale data between $[0, 1]$, zero mean normalization proved more effective based on our experiments. Following normalization, the dataset is divided into training and testing sets in an 8:2 ratio, with ten percent of the training data allocated for validation during the training process. Validation is crucial for assessing the model's learning status, identifying over-fitting, under-fitting, or optimal learning. Subsequently, a loss function is designed, with the choice being the *Binary Cross-Entropy (BCE) loss*, which is a classic loss function for classification problems. Before training, hyperparameters and optimizer settings are configured as detailed in Section V-A. The optimal MLP model training process is presented in Figure 3, showing a consistent decrease in both training loss and validation losses indicated successful learning. The Accuracy metric, which calculates the ratio between the number of

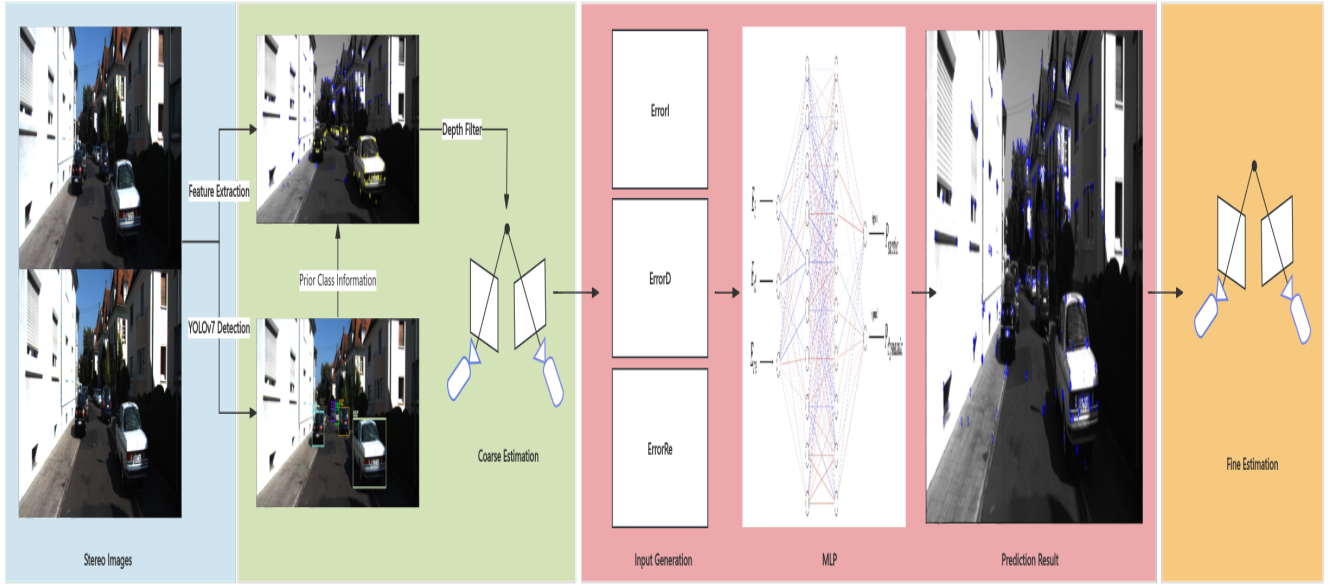


Fig. 2. Diagram of our proposed MLP based real-time stereo SLAM system. There are four main parts in total. The blue section involves pre-processing, feature extraction, object detection, and object tracking. The green section is for coarse estimation, generating a rough pose estimation. The pink section involves an MLP model for classifying dynamic and static feature points within potential dynamic objects. The yellow section is for fine estimation, refining the camera pose generated in the coarse estimation stage by minimizing the re-projection error of all static feature points. These points include those outside the bounding box of potential dynamic objects, filtered by the Depth Filter Module, and classified as static by the MLP model.

correct classification cases and the number of total cases, is shown to be increasing.

The MLP prediction module begins by generating input feature v_i for each feature point x_i that is located in the bounding box and is not filtered by Depth Filter Module, then normalizing the input feature v_i through zero mean normalization to eliminate dimension effects, using the same parameters as the dataset normalization. Finally, all input features are put into the model in packs of a predetermined size and are classified as static or dynamic.

D. Fine Estimation

Upon utilizing the MLP model to classify feature points, we are able to differentiate between static and dynamic feature points located within the bounding box of all objects. Subsequently, feature points outside the bounding box, as well as static points filtered by the Depth Filter and classified as static by the MLP, are combined to form a comprehensive set of static feature points. During the fine estimation phase, the camera pose initially generated in the coarse estimation stage is refined by minimizing the re-projection error of the static feature points.

E. Data Collection

For an extended period, there has been a lack of publicly available datasets for directly evaluating dynamic and static feature points classification methods. Currently, all methods are assessed indirectly through SLAM metrics, which can lead to inaccuracies and instability as it overlooks the randomness inherent in the SLAM system. For bridging this gap, we build a publicly available datasets which contains over

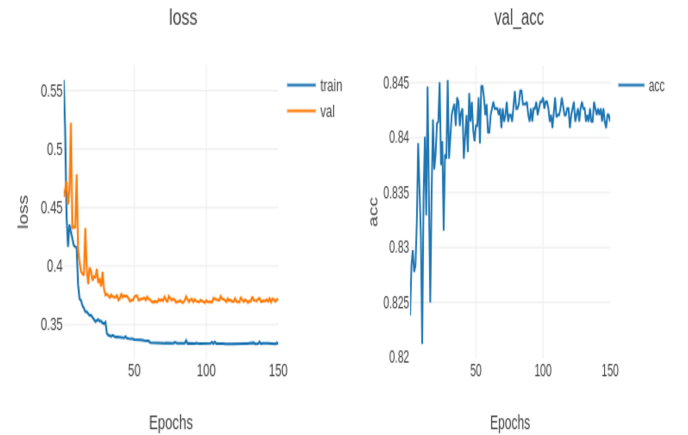


Fig. 3. Training process of optimal MLP model. It is showing a consistent decrease in both training loss and validation losses indicated successful learning. Also, the Accuracy metric, which calculates the ratio between the number of correct classification cases and the number of total cases, is shown to be increasing.

50,000 dynamic and static feature points from sequences 00 and 01 of KITTI tracking datasets. Each feature points is saved as following format, $u_1, v_1, z_1, id_1, u_2, v_2, id_2, class, e_I, e_{Re}, e_D$. The $(u_1, v_1), (u_2, v_2)$ stands for coordinates of feature point x_1 and x_2 in image frame respectively. And z_1 means the depth of x_1 , which is computed through the same way as in ORB-SLAM2. The id_1 and id_2 represent whether the image frames belong to x_1 or x_2 . The $class$ is binary, either *dynamic* or *static*. The most important properties are e_I, e_{Re} and e_D , and they represent image intensity error,

re-projection error and epipolar error respectively. We use ground truth pose of each frame to generate them. Details of how they are computed is represented in formulas (3), (4) and (5).

V. EXPERIMENTAL RESULTS

A. Experimental Settings

A C++-implemented MLP-based real-time stereo SLAM system is tested on a laptop with an Intel Core i9-13900k@5.8 GHz processor. The YOLOv7 and DeepSort are used to detect object class, locate 2D bounding boxes, and track objects. Both of them are executed on an Nvidia RTX3080 GPU, and the rest of the SLAM system runs on the CPU.

Parameter η in *Depth Filter Module* is set to 1.2. Parameters related to the training part of the MLP model are as follows: the *epoch* is 150, the *batch size* is 8, the *learning rate* is 0.1, the *learning rate scheduler* is *MultiStepLR* [25] with γ set to 0.1. The optimizer we choose is *Adam* [26]. We converted the TensorRT [27] version of the MLP model with a fixed input shape of (200, 3).

TABLE I
CLASSIFICATION COMPARISON

Method	Accuracy	F1-Score
MLP	87.71	87.64
SVM	84.19	84.58
method similar to PointSLOT	81.36	81.43
method similar to CFP-SLAM	73.61	71.10
e_D only	50.62	51.32

B. Classification Evaluation

As previously stated, we have compiled a dataset for classifying dynamic and static feature points, consisting of over 50,000 feature points. This dataset enables the direct evaluation of various dynamic and static feature classification methods, eliminating the need for indirect comparisons based on metrics from the SLAM field. Direct evaluation is advantageous as it is less influenced by other factors within the SLAM system, resulting in more reliable and accurate experimental outcomes.

Our experiment involves the assessment of various methods for feature discrimination, including our MLP based dynamic and static feature discriminator, Support Vector Machine (SVM), a method akin to PointSLOT, a method similar to CFP-SLAM, and a method focusing solely on epipolar error. SVM is a well-established classification technique in machine learning, widely used in text and hypertext categorization, image classification, and satellite data classification. In this study, SVM from the Scikit-learn library [28] is directly employed, trained, and evaluated on the dataset. Additionally, two classification methods for dynamic and static feature points, similar to PointSLOT and CFP-SLAM, are implemented in Python due to the unavailability of their source code. The PointSLOT solely focuses on re-projection

error, while the CFP-SLAM considered epipolar error in addition. Furthermore, a discrimination method concentrating solely on epipolar error is also implemented. The evaluation of these methods is based on the metrics of Accuracy and F1-score. Accuracy reflects the model’s predictive correctness, with true positive (TP), false positive (FP), true negative (TN), and false negative (FN) used to denote classification outcomes.. And the Accuracy is described as following:

$$\text{Accuracy} = \frac{TP + TN}{TP + FP + TN + FN} \quad (9)$$

The F1-Score is a measure of the predictive performance of the model. It is the harmonic mean of the Precision and Recall. The Precision and Recall indicated correct identified proportion of positive identifications and correct proportion of actual positives respectively. Thus, the F1-Score symmetrically represents both precision and recall in one metric. It can be described as follows

$$\text{F1-Score} = \frac{2 \times \text{Precision} \times \text{Recall}}{\text{Precision} + \text{Recall}} \quad (10)$$

$$\text{Precision} = \frac{TP}{TP + FP} \quad (11)$$

$$\text{Recall} = \frac{TP}{TP + FN} \quad (12)$$

The experimental results are presented in Table I. According to Table I, we can see that our MLP-based dynamic and static feature points discriminator achieves superior performance in terms of both Accuracy and F1-Score compared to other methods. Additionally, the support-vector machine (SVM) outperforms other methods except for our MLP-based method. Both MLP and SVM belong to machine learning methods, indicating that machine learning-based methods are more suitable for this dynamic and static feature classification problem compared to traditional methods that require manual parameter tuning. The significant difference between the method that only considers epipolar error and the method similar to PointSLOT which only considers re-projection error, suggests that re-projection error is a more critical indicator than epipolar error for this problem.

C. Visual Odometry

KITTI tracking dataset is a publicly available collection of stereo visual odometry datasets. It comprises 11 training sequences and 10 testing sequences featuring urban and road scenes captured from a car’s perspective, including moving vehicles, along with corresponding GPS data.

We conduct a comprehensive comparison between our MLP-based SLAM system and other SLAM systems in this section. Table II presents a detailed comparison result. In Table II, we provide an absolute translation error (ATE) comparison with ORB-SLAM2, DynaSLAM, DynaSLAM II, and a modified version of VDO-SLAM. ORB-SLAM2 does not specifically address dynamic situations but serves as the foundation of our SLAM system. DynaSLAM also builds upon ORB-SLAM2 with the ability to detect dynamic objects, but it discards features located within the

TABLE II
THE ATE COMPARISON ON KITTI DATASETS

Sequences	ORB-SLAM2	DynaSLAM	DynaSLAM II	VDO-SLAM	us
00	0.91	1.40	1.29	–	0.79
01	7.35	9.40	2.31	189.13	4.53
02	3.36	6.70	0.91	–	3.48
03	0.39	0.60	0.69	5.36	0.34
04	0.15	0.20	1.42	3.46	0.24
05	0.54	0.80	1.34	–	0.33
06	0.44	0.80	0.19	3.63	0.88
07	0.42	0.50	3.30	2.73	0.41
08	3.03	3.50	1.68	–	3.18
09	3.97	1.60	5.02	11.73	0.90
10	1.34	1.30	1.30	3.72	1.27
average	1.99	2.43	1.77	–	1.48

bounding box of potential dynamic objects directly, leading to information loss. DynaSLAM II is the current state-of-the-art method, aiming to enhance camera pose estimation precision by optimizing the Bundle Adjustment (BA) factor graph, which includes object poses and constant velocity constraints. The modified version of VDO-SLAM [29] is a re-implemented version; the original version can only run on datasets provided by the authors. The modified VDO-SLAM requires acquiring depth images through ZoeDepth [30], optical flow through VideoFlow offline, and applying YOLOv8 [31] to detect dynamic objects. We tested all SLAM systems on our experimental devices except DynaSLAM II due to the unavailability of its source code. Therefore, we directly used the experimental results from its original paper.

According to experimental results in Table II, it can be seen that our SLAM system outperforms other SLAM system in most of sequences of Kitti tracking datasets. More specifically, our SLAM system outperforms VDO-SLAM-modified version in all sequences. Besides, compared to our base ORB-SLAM2, we achieve better performance in the sequences 00, 01, 03, 05, 07, 08, 09 and 10. The sequence 01 is collected from a car driving on the high way, where all cars that show up at this sequence are dynamic. Our SLAM system works better than ORB-SLAM2 in this sequence, which indicates that our SLAM system has the ability to address dynamic objects in the surrounding environment correctly. Moreover, compared to DynaSLAM, our SLAM system achieves higher precision on sequences except for sequences 04 and 06, and the gap on the sequence 04 and 06 are within 0.1. Compared to DynaSLAM II, our SLAM system only performs worse on the sequences 01, 02, 06 and 08 out of 11 sequences. However, our SLAM system achieved lowest average absolute translation error (ATE). It indicates that our SLAM system achieves the highest average precision over all sequences of Kitti tracking dataset. It is worth mentioning that the sequence 00 is rich of static cars that are parked on the roadside, our SLAM system achieves the best performance in this sequence compared to other methods, which indicates that our MLP model is capable to identifying real dynamic objects.

TABLE III
LATENCY OF EACH MODULE

Module	ORB-SLAM2 (stereo)	us
Feature Process	37.31 ms	37.61 ms
Pose Estimation	1.78 ms	2.58 ms
YOLOv7 Detection	–	7.72 ms
Deep Sort Tracking	–	4.66 ms
MLP Inference	–	0.18 ms
Tracking	45.31 ms	62.81 ms

D. Time Analysis

Low latency is one of the desired property of the SLAM system. Most of onboard devices are not capable of executing tasks with high computation cost. We lists the average computational time of each module in the tracking thread of our MLP based stereo SLAM system in Table III. According to experimental results from Table II and Table III, our MLP-based SLAM system achieves higher precision with only 17.50ms/frame extra computation cost. Moreover, we made a comprehensive latency comparison with other SLAM systems. The mean values of the highest latency and the lowest latency from the original papers of DynaSLAM II and PointSLOT are presented in Table IV. For all other methods in Table IV, average latency value in Kitti tracking sequences from 00 to 10 are presented. It is worth mentioning that even though the latency of DynaSLAM II does not include the time consumption of 2d and 3d object detection models, the execution time of our methods is still 17.34ms faster. Combining Table II and Table IV, we can conclude that our MLP-based SLAM system achieves the lowest average absolute translation error (ATE) and the fastest speed compared to other dynamic SLAM systems.

VI. CONCLUSIONS

In this letter, we propose a MLP-based real-time stereo SLAM system to address SLAM system degradation in dynamic environments. Currently, there is no publicly available dataset for directly evaluating the effectiveness of dynamic

TABLE IV
LATENCY ANALYSIS

Method	Sensor	Latency
ORB-SLAM2	Stereo	45.31 ms (base)
DynaSLAM	Stereo	519.37 ms
DynaSLAM II	Stereo	80.15 ms
VDO-SLAM	Stereo + Dpeth	86.97 ms
PointSLOT	Stereo	73.6 ms
us	Stereo	62.81 ms

and static feature classification methods. Previous assessments have relied on indirect metrics, which are prone to inaccuracy due to the randomness in the Random Sample Consensus (RANSAC) process in camera pose estimation within the SLAM systems. To bridge this gap, we have created a publicly available dataset containing over 50,000 feature points. Our proposed MLP-based dynamic and static feature discriminator is the most effective method compared to other methods on our collected datasets. Additionally, our MLP-based real-time stereo SLAM system achieves the highest average precision on the KITTI tracking dataset and the fastest speed compared to other dynamic SLAM systems.

ACKNOWLEDGMENT

We would like to acknowledge the subaward from the Virginia Tech under the U.S. Army Grant No. W911QX-23-2-0001.

REFERENCES

[1] R. Mur-Artal and J. D. Tardós, “Orb-slam2: An open-source slam system for monocular, stereo, and rgb-d cameras,” *IEEE Transactions on Robotics*, vol. 33, no. 5, pp. 1255–1262, 2017.

[2] C. Campos, R. Elvira, J. J. G. Rodríguez, J. M. Montiel, and J. D. Tardós, “Orb-slam3: An accurate open-source library for visual, visual-inertial, and multimap slam,” *IEEE Transactions on Robotics*, vol. 37, no. 6, pp. 1874–1890, 2021.

[3] J. Engel, T. Schöps, and D. Cremers, “Lsd-slam: Large-scale direct monocular slam,” in *European conference on computer vision*. Springer, 2014, pp. 834–849.

[4] J. Engel, V. Koltun, and D. Cremers, “Direct sparse odometry,” *IEEE transactions on pattern analysis and machine intelligence*, vol. 40, no. 3, pp. 611–625, 2017.

[5] Z. Zhu, S. Peng, V. Larsson, W. Xu, H. Bao, Z. Cui, M. R. Oswald, and M. Pollefeys, “Nice-slam: Neural implicit scalable encoding for slam,” in *Proceedings of the IEEE/CVF conference on computer vision and pattern recognition*, 2022, pp. 12 786–12 796.

[6] B. Bescos, J. M. Fácil, J. Civera, and J. Neira, “DynaSLAM: Tracking, mapping, and inpainting in dynamic scenes,” *IEEE Robotics and Automation Letters*, vol. 3, no. 4, pp. 4076–4083, 2018.

[7] A. Geiger, P. Lenz, C. Stillér, and R. Urtasun, “Vision meets robotics: The kitti dataset,” *The International Journal of Robotics Research*, vol. 32, no. 11, pp. 1231–1237, 2013.

[8] X. Hu, Y. Zhang, Z. Cao, R. Ma, Y. Wu, Z. Deng, and W. Sun, “Cfp-slam: A real-time visual slam based on coarse-to-fine probability in dynamic environments,” in *2022 IEEE/RSJ International Conference on Intelligent Robots and Systems (IROS)*. IEEE, 2022, pp. 4399–4406.

[9] P. Zhou, Y. Liu, and Z. Meng, “Pointslot: Real-time simultaneous localization and object tracking for dynamic environment,” *IEEE Robotics and Automation Letters*, vol. 8, no. 5, pp. 2645–2652, 2023.

[10] J. Zhang, M. Henein, R. Mahony, and V. Ila, “Vdo-slam: A visual dynamic object-aware slam system,” *arXiv preprint arXiv:2005.11052*, 2020.

[11] S. Wen, X. Li, X. Liu, J. Li, S. Tao, Y. Long, and T. Qiu, “Dynamic slam: A visual slam in outdoor dynamic scenes,” *IEEE Transactions on Instrumentation and Measurement*, 2023.

[12] G. Jocher, A. Chaurasia, A. Stoken, J. Borovec, Y. Kwon, K. Michael, J. Fang, Z. Yifu, C. Wong, D. Montes, *et al.*, “ultralytics/yolov5: v7.0-yolov5 sota realtime instance segmentation,” *Zenodo*, 2022.

[13] D. Bolya, C. Zhou, F. Xiao, and Y. J. Lee, “Yolact: Real-time instance segmentation,” in *Proceedings of the IEEE/CVF international conference on computer vision*, 2019, pp. 9157–9166.

[14] C. Yu, Z. Liu, X.-J. Liu, F. Xie, Y. Yang, Q. Wei, and Q. Fei, “Ds-slam: A semantic visual slam towards dynamic environments,” in *2018 IEEE/RSJ international conference on intelligent robots and systems (IROS)*. IEEE, 2018, pp. 1168–1174.

[15] K. He, G. Gkioxari, P. Dollár, and R. Girshick, “Mask r-cnn,” in *Proceedings of the IEEE international conference on computer vision*, 2017, pp. 2961–2969.

[16] M. Ester, H.-P. Kriegel, J. Sander, X. Xu, *et al.*, “A density-based algorithm for discovering clusters in large spatial databases with noise,” in *kdd*, vol. 96, no. 34, 1996, pp. 226–231.

[17] B. Bescos, C. Campos, J. D. Tardós, and J. Neira, “DynaSLAM ii: Tightly-coupled multi-object tracking and slam,” *IEEE robotics and automation letters*, vol. 6, no. 3, pp. 5191–5198, 2021.

[18] F. Rosenblatt, “Principles of neurodynamics. perceptrons and the theory of brain mechanisms,” Cornell Aeronautical Lab Inc Buffalo NY, Tech. Rep., 1961.

[19] Y. LeCun, L. Bottou, Y. Bengio, and P. Haffner, “Gradient-based learning applied to document recognition,” *Proceedings of the IEEE*, vol. 86, no. 11, pp. 2278–2324, 1998.

[20] A. Rana, A. S. Rawat, A. Bijalwan, and H. Bahuguna, “Application of multi layer (perceptron) artificial neural network in the diagnosis system: a systematic review,” in *2018 International conference on research in intelligent and computing in engineering (RICE)*. IEEE, 2018, pp. 1–6.

[21] E. Sucar, S. Liu, J. Ortiz, and A. J. Davison, “imap: Implicit mapping and positioning in real-time,” in *Proceedings of the IEEE/CVF international conference on computer vision*, 2021, pp. 6229–6238.

[22] M. Li, J. He, Y. Wang, and H. Wang, “End-to-end rgb-d slam with multi-mlps dense neural implicit representations,” *IEEE Robotics and Automation Letters*, 2023.

[23] C.-Y. Wang, A. Bochkovskiy, and H.-Y. M. Liao, “Yolov7: Trainable bag-of-freebies sets new state-of-the-art for real-time object detectors,” in *Proceedings of the IEEE/CVF conference on computer vision and pattern recognition*, 2023, pp. 7464–7475.

[24] Y. Du, Z. Zhao, Y. Song, Y. Zhao, F. Su, T. Gong, and H. Meng, “Strongsort: Make deepsort great again,” *IEEE Transactions on Multimedia*, vol. 25, pp. 8725–8737, 2023.

[25] A. Paszke, S. Gross, F. Massa, A. Lerer, J. Bradbury, G. Chanan, T. Killeen, Z. Lin, N. Gimelshein, L. Antiga, *et al.*, “Pytorch: An imperative style, high-performance deep learning library,” *Advances in neural information processing systems*, vol. 32, 2019.

[26] D. Kingma, “Adam: a method for stochastic optimization,” *arXiv preprint arXiv:1412.6980*, 2014.

[27] N. Corporation, “Nvidia tensorrt,” <https://docs.nvidia.com/deeplearning/tensorrt/sla/index.html#supplement>, 2015.

[28] F. Pedregosa, G. Varoquaux, A. Gramfort, V. Michel, B. Thirion, O. Grisel, M. Blondel, P. Prettenhofer, R. Weiss, V. Dubourg, *et al.*, “Scikit-learn: Machine learning in python,” *the Journal of machine Learning research*, vol. 12, pp. 2825–2830, 2011.

[29] Ituring, “Vdo-slam modified version,” https://github.com/Ituring/VDO-SLAM_modified, 2024.

[30] S. F. Bhat, R. Birkl, D. Wofk, P. Wonka, and M. Müller, “Zoedepth: Zero-shot transfer by combining relative and metric depth,” *arXiv preprint arXiv:2302.12288*, 2023.

[31] G. Jocher, A. Chaurasia, and J. Qiu, “Ultralytics YOLO,” Jan 2023. [Online]. Available: <https://github.com/ultralytics/ultralytics>